A Blur Kernel Estimation Method Based on the Multiplicative Multiresolution Decomposition (MMD)

Fatma Kerouh and Amina Serir
U.S.T.H.B, L.T.I.R, Faculté d'Electronique et d'Informatique
B.P. 32 El Alia Bab Ezzouar, Alger 16111, Algérie.
E-mail: f.kerouh@usthb.dz, aserir@usthb.dz

***Abstract*—The aim of this article is to propose a blur kernel estimation method based on the new concept of the Multiplicative Multiresolution Decomposition (MMD). This method quantifies the blur effect in the MMD's domain by analyzing edges spreading through a multiresolution analysis. The histogram of edges spreading over the entire image is used as information about the blur amount in the image. Tests on blurred images from the LIVE database show that, the proposed approach provides an accurate blur kernel estimation.**

***Index Terms*—blurring, edges, blind deconvolution, the Multiplicative Multiresolution Decomposition, the wavelet transform**

I. Introduction

In many imaging applications, an observed image *g(x, y),* could be estimated to be the two dimensional convolution of the true image *f (x, y)* with a linear shift-invariant blur, also known as the Point Spread Function (PSF), *h (x, y),* plus an added noise *n (x, y).* That is,

$$g(x,y)=f(x,y)*h(x,y)+n(x,y)\ . \qquad (1)$$

In which * denotes the two dimensional linear convolution operator. The problem of recovering the true image *f (x, y)* requires the deconvolution of the PSF *h (x, y)* from the degraded image *g (x, y).*

Deconvolution is performed for image restoration in many applications such as astronomical speckle imaging, remote sensing and medical imaging, among others. In most situations, the PSF *h (x, y)* is assumed to be known explicitly prior to the deconvolution procedure. This problem is known as the classical linear image restoration problem. The long list of deconvolution methods for this situation includes a variety of well known techniques, such as inverse filtering, Wiener filtering, least squares filtering, recursive Kalman filtering and constrained iterative deconvolution methods [1], [2], [3]. Unfortunately, in many practical situations, the blur kernel is often unknown, such an estimation problem assuming the linear degradation model of eq. 1, is called blind deconvolution. To resolve such problem, we propose to identify the PSF separated from the true image, in order to use it later with one of the known classical image restoration methods. Estimating the PSF and the true image are disjoint procedures. This approach leads to computationally simple algorithms.

Blurring could be defined locally as a multiplicative noise; it affects especially edges which represent the high frequency component of an image. Therefore, edge detection is a common step in most blurred image characterization methods. It exists in the literature several approaches for edge detection, for instance Gradient based methods [4], [5]. The multi-resolution decomposition especially the Wavelet transform has proven to be an efficient tool for edge extraction [6]. This study is focused on edge detection with a multiscale singularity analysis using the new concept of a Multiplicative Multiresolution Decomposition (MMD). The MMD is an effective normalized decomposition for edge detection since it produces significant coefficients precisely where the image intensity varies (edges). This multiplicative transform seems to be more suitable for the blur effect characterization. A comparison of the MMD and the Wavelet transform performance is done.

This paper is organized as follows. The Multiplicative Multiresolution Decomposition concept is presented in section 2. Section 3 introduces the proposed approach for blurred image characterization. Experimental results and discussions are presented in section 4. The last section concludes this work with some perspectives.

II. The Multiplicative Multiresolution Decomposition Concept

A new method is adopted to deal directly with our purpose. The MMD transform is applied on blurred images to extract all blurred edges and singularities.

A. The Multiplicative Decomposition

A nonlinear multiplicative decomposition using filter banks with critical sub-sampling and perfect reconstruction is presented in [7], [8]. The bi-dimensional extension of this transform [8], [9] is defined as follows. Let us consider a description of the analysis and synthesis inputs–outputs systems with equal symbol rates at both the input and the output (Fig. 1 and Fig. 2). The wanted structure is obtained by performing a polyphase

Manuscript received February 8, 2013; revised April 10, 2013.

doi: 10.12720/joig.1.2.104-108

decomposition of the 2D signal (image). The four polyphase components x_{11}, x_{12}, x_{21} and x_{22} of the input image $I(n, m)$ are defined by:

$$\forall (i,j) \in \{1,2\},\quad x_{ij}(n,m) = I(2(n-1)+i, 2(m-1)+j). \tag{2}$$

The linear filters h_{ij} and f_{ij} are defined as:

$$\forall (i,j) \in \{1,2\},\quad h_{ij}(n,m) = h(2(k+1)+i, 2(l+1)+j). \tag{3}$$

$$f_{ij}(n,m) = f(2(k+1)+i, 2(l+1)+j). \tag{4}$$

where, h and f are the bi-dimensional linear filters. Let's consider D and r_{ij}, $i,j \in \{1,2\}$, the analysis and synthesis nonlinear filters , respectively. Fig. 1, Fig. 2 show the analysis and synthesis bi-dimensional multiplicative nonlinear filter banks with polyphase scheme. According to Fig. 1 and Fig. 2, and for a perfect reconstruction, we need to have $\hat{x}_{ij} = x_{ij}$.

Let us set:

$f_{11} = h_{11}^{-1}, f_{12} = h_{12}^{-1}, f_{21} = h_{21}^{-1}, f_{22} = h_{22}^{-1}, h_{12} = \alpha h_{11}$, $h_{21} = \mu h_{11}$ and $h_{22} = \gamma h_{11}$ where α, μ, γ are positive scalars.

The nonlinear analysis filter D is then given by:

$$y_{2v} = \begin{cases} \beta \dfrac{x_{12}}{x_{11}}, & for\ x_{11} = x_{12}, \\ \beta \left(2 - \dfrac{x_{11}}{x_{12}}\right), & for\ x_{12} > x_{11}, \\ \alpha, & for\ x_{12} = x_{11} = 0. \end{cases} \tag{5}$$

$$y_{2h} = \begin{cases} \beta \dfrac{x_{21}}{x_{11}}, & for\ x_{11} = x_{21}, \\ \beta \left(2 - \dfrac{x_{11}}{x_{21}}\right), & for\ x_{21} > x_{11}, \\ \mu, & for\ x_{21} = x_{11} = 0. \end{cases} \tag{6}$$

$$y_{2d} = \begin{cases} \beta \dfrac{x_{22}}{x_{11}}, & for\ x_{11} = x_{22}, \\ \beta \left(2 - \dfrac{x_{11}}{x_{22}}\right), & for\ x_{22} > x_{11}, \\ \gamma, & for\ x_{22} = x_{11} = 0. \end{cases} \tag{7}$$

for $x_{11} \neq 0$, the following nonlinear filters r_{ij} could be deduced

$$r_{11}(y_{2h}, y_{2v}, y_{2d}) = \frac{1}{1+\alpha\frac{x_{12}}{x_{11}}+\mu\frac{x_{21}}{x_{11}}+\gamma\frac{x_{22}}{x_{11}}}. \tag{8}$$

$$r_{12}(y_{2h}, y_{2v}, y_{2d}) = \propto \frac{x_{12}}{x_{11}} r_{11}(y_{2h}, y_{2v}, y_{2d}). \tag{9}$$

$$r_{22}(y_{2h}, y_{2v}, y_{2d}) = \gamma \frac{x_{22}}{x_{11}} r_{11}(y_{2h}, y_{2v}, y_{2d}). \tag{10}$$

Here β is a positive scalar fixed at 0.5. Hence, for $x_{11} \neq 0$ (equivalent to have, $y_{2h} \neq \mu$ and $y_{2v} \neq \gamma$, according to equations (8, 9 and 10), the nonlinear filters r_{ij} are expressed as a function of the nonlinear outputs y_{2h}, y_{2v}, y_{2d}.

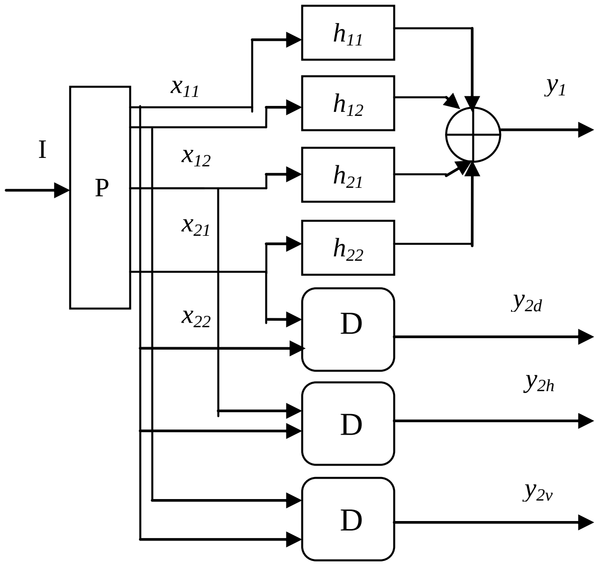

Figure 1. An analysis non-linear filter bank based on MMD

P : polyphase decomposition

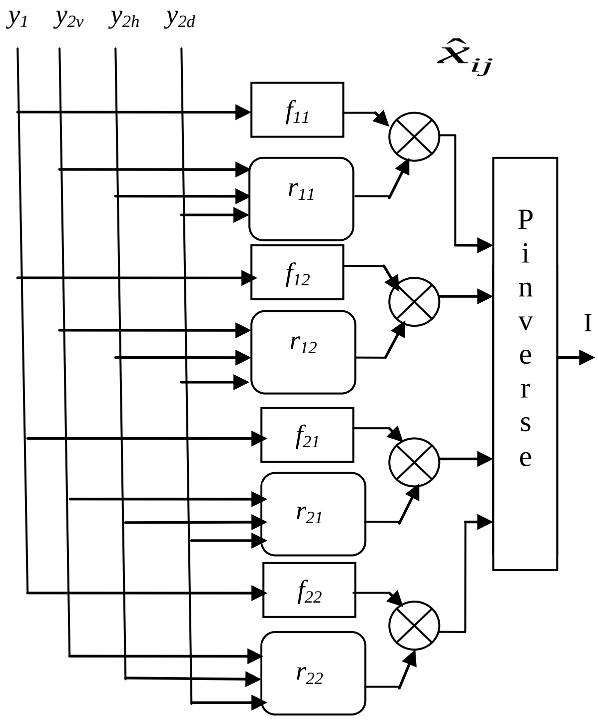

Figure 2. A synthesis nonlinear filter bank based on MMD

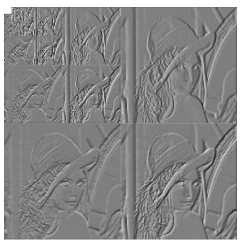

Figure 3. MMD multiresolution analysis for $J=5$.

B. Multiresolution Multiplicative Decomposition

Several sub-band decompositions are cascaded by applying the analysis filter banks to one or more coefficients outputs of the preceding stage. Herein, we consider the frequent case where the approximation sub-band is re-decomposed (according to Fig. 1, we assume that the sub-band y_1 corresponds to the approximation sub-band). The sub-band y_1 is split to its polyphase components $y_{11}, y_{12}, y_{21}, y_{22}$ and then filtered. Consider, at the resolution *j=1*, that, $y_{11}^{(j)} = x_{11}$, $y_{12}^{(j)} = x_{12}$, $y_{21}^{(j)} = x_{12}$ and $y_{22}^{(j)} = x_{22}$. Thus, for any *J>0*, the original discrete signal $y_1^{(1)} = I$ measured at the resolution 1 is represented by the set S.

$$S = \left(y_1^{(J)}, (y_{2h}^{(j)}, y_{2v}^{(j)}, y_{2d}^{(j)}\right)_{2\leq j\leq J}. \quad (11)$$

Inversely, an approximation of the reconstructed signal at resolution *j=1* is obtained by using multi-resolution synthesis sub-band and the representation of the set of signals S.

III. Proposed Method

The proposed approach is based on studying the histogram of the detected edge pixels spreading through a multiresolution analysis using the MMD. The proposed approach could be explained in three main steps. First edge pixels are extracted at each resolution level using the MMD, and then the spreading out of each detected edge pixel is estimated. Finally an analysis and an interpretation of the obtained values are made.

A. Edge Detection

Apply the MMD decomposition at three resolutions to extract detail images (Fig. 3). To reduce the noise effect and for a better edge pixel extraction, an adequate threshold at each resolution level "*j",* is applied on the detail images as follows:

$$y_{2c}(k,l) = \begin{cases} y_{2c}(k,l) \; if \; y_{2c}(k,l) > Th_j \,, \\ \beta \qquad otherwise \,. \end{cases} \quad (12)$$

$with \;\; Th_j = \beta \times j + m_j.$

The subscript *'c'* denotes the horizontal, '*H*', vertical '*V*', or diagonal '*D*' details obtained from the MMD.

By studying the MMD's detail coefficients at different resolutions, we found that it is useful to define a threshold value Th_j relying on the resolution level j and m_j the mean value of the obtained details at each resolution level defined as follows.

$$m_j = \frac{1}{N_j \times M_j} \sum_{k=1}^{k=N_j} \sum_{l=1}^{l=Mj} y_{2c}^{(j)}(k,l) \quad (13)$$

here N_j *and* M_j , represents the number of rows and columns respectively of the MMD's image detail at each resolution level *j*.

B. Estimate the detected edge pixels spreading out values

The width around the edge pixel is measured in the MMD's domain, it's corresponds to the number of pixels with the MMD's coefficient values different from β. For each detail image at each direction (horizontal, vertical and diagonal), the spreading out of each detected edge pixel is computed following the orthogonal direction. The width is then computed as the sum of both counts excluding the edge pixel.

C. An analysis Step

Having information about the total number of edge pixels and their spreading values, the objective now is to analyze the obtained information. For the analysis, the maximum spreading out value in the three directions (horizontal, vertical or diagonal) is only considered. The histogram of the detected edge pixels spreading values at each resolution level is then constructed. Finally the spreading out mean value is chosen as the considered image blur kernel.

This applies when it is assumed that the blur is globally over the entire image. However having the information at each edge point about the spread, could be adapted to the local blur problem.

IV. Experiments and Results

The proposed method performance has been evaluated on the Live database images from Texas University, containing Gaussian blurred images (Gblur). This database comprises a set of twenty-nine original images, high-resolution (24 bits/pixel) in RGB colors (Fig. 4). All these original images are filtered using a circular-symmetric 2-D Gaussian kernel of standard deviation ranging from 0.42 to 15 pixels, which results in a set of 174 stimuli [10]-[12].

To show the proposed method effectiveness, let's consider from the LIVE database one original image and its blurred version represented in Fig. 5. To evaluate blurred images quality, a no reference metric (*IQA*) developed in [13] is considered. While computing the edges width of the entire images using the proposed algorithm, the obtained results are shown in Fig. 6. The obtained edge spreading values (ESV) of the original and the blurred images are, 1.023 and 2.834, respectively. According to Fig. 6, it could be clearly noticed that the edges spreading out are more important in the blurred image compared to the clearest one. Indeed blurring affects especially edges and makes transitions spreading larger. However in clearer images, transitions are sharp and edges spreading out are narrower.

While applying the proposed algorithm on all Live dataset images (174 images), the obtained mean Spreading out value of each image is evaluated against its objective quality score representing the Standard Deviation value of the Gaussian function introducing blur in this image. The obtained results are presented in Fig. 7. In addition, the estimated blur kernel for each image is tested against its blur quality measure using the no reference blur image quality measure developed in [13]. The obtained results are represented in Fig. 8.

For data fitting a Logistic regression has been considered. It is defined in (14).

Figure 4. Live dataset original images

(a) (b)
IQA(a)=0.9827 IQA(b)=0.6725

Figure 5. .Test images, (a) Clear images, (b) blurred version

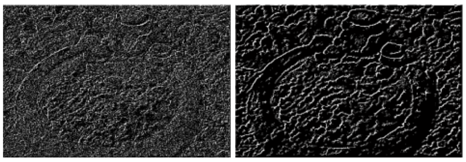

(a) (b)

Figure 6. The detected edges spreading out of, (a) Clear image, (b) Blurred version

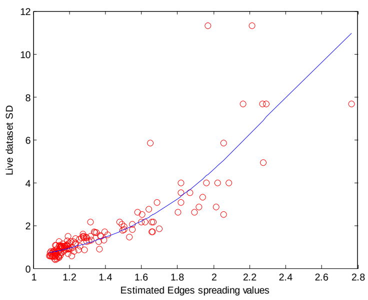

Figure 7. Scatter plot of the Estimated ESV versus SD values

SROOC= 0.9138, RMSE= 0.9595

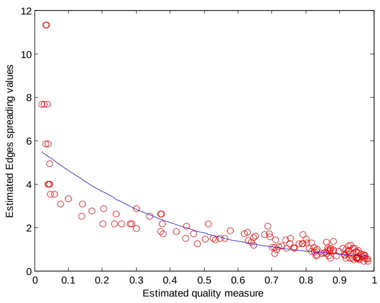

Figure 8. A scatter plot of the Estimated ESV versus the obtained quality measure values

SROCC = 0.9273, RMSE =0.9590

$$ESV_i = \frac{\alpha_1 - \alpha_2}{1 + e^{\frac{SD_i - \alpha_3}{|\alpha_4|}}} + \alpha_2 \qquad (14)$$

where α_1, α_2 , α_3 *and* α_4 are the logistic parameters, ESV_{pi} is the predicted Spreading value of the image i, and SD_i is the given Standard Deviation value of the considered image i. To appreciate the obtained interpolation model, a Spearman Rank Order Correlation Coefficient (SROCC) is used.

$$SROCC = 1 - \frac{\sum D^2}{n(n^2 - 1)} \qquad (15)$$

D is the difference between interpolating model and samples and n is the total number of samples.

The Root Mean Square Error (RMSE), is also computed to evaluate the obtained interpolation model. The evaluation of Fig.s 7 and 8 revealed a high Spearman correlation value between the interpolation model and the obtained samples (more than 90%) for a small Root Mean Square Error (less than 1).

From the obtained results, one could conclude that the proposed algorithm for blur kernel estimation provides an accurate estimation especially for slightly and averagely blurred images. According to Fig. 7, it could be noticed that for the heavily blurred images ($SD \geq 8$), as the images represented in Fig. 9, the proposed method is less accurate. This is due to the difficulty to extract edge pixels because the blur effect smoothes enormously images.

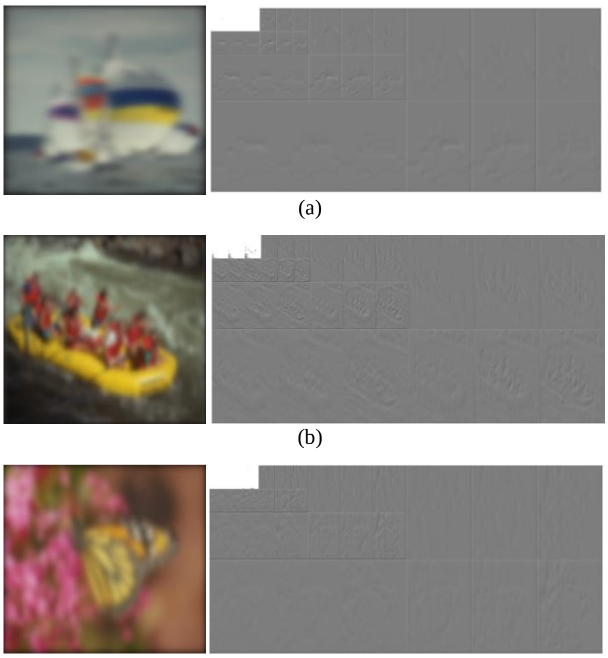

(a) (b) (c)

Figure 9. Heavily blurred images and their MMD's details at three resolutions

($\sigma_{(a)}$ =11.333325 , $\sigma_{(b)}$ =7.666650, $\sigma_{(c)}$ =11.333325)
IQA(a)=0.2323, IQA(b)=0.2590, IQA(c)=0.2367

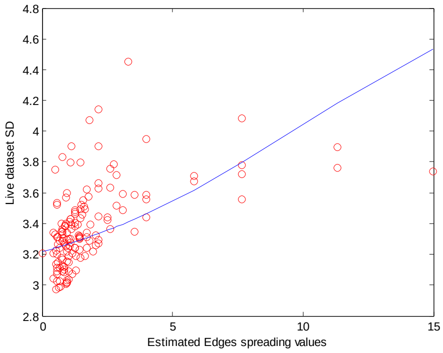

Figure 10. A scatter plot of the estimated ESV versus SD values using the Wavelet transform

SROOC= 0.6436, RMSE= 0.2236

For a comparative study, the same methodology has been adopted using the Wavelet transform. The obtained blur kernel values evaluation against the standard deviation values of all the Live dataset images are shown in Fig. 10. Accordingly, the results are less accurate in terms of the Spearman correlation as well as the Mean Square Error. The obtained results are accepted only for slightly blurred images (*SD<2*). In fact the MMD is well adapted due to its multiplicative aspect and its normalized coefficients.

V. Conclusion

In this work, an algorithm for blur kernel estimation based on the new concept of the MMD was presented. Our tests using the Live database show that the proposed approach revealed encouraging results. The multiresolution analysis using the MMD transform allows effectively a good blur effect characterization. As perspective for future work, we prospect to develop a blind deconvolution algorithm using the proposed estimated blur kernel.

References

[1] A. K. Jain and S. Ranganath, “Applications of two dimensional spectral estimation in image restoration,” in *Proc. IEEE Int Conf Acoustics, Speech, Signal Processing*, 1981, pp. 1113-1116.

[2] J. Biemond, R. L. Lagendijk, and R.M. Mersereau, “Iterative methods for image deblurring,” *IEEE*, vol. 78, no. 5, pp. 856-883, May 1990.

[3] A. O. Aboutalib and L. M. Silverman, “Restoration of motion degraded images,*”IEEE Trans Cir Sys, CAS-22*, pp. 278-286, March 1975.

[4] M. G. Choi, J. H. Jung, and J. W. Jeon, “No-reference image quality assessment using blur and noise,” *Word Academy of Science, Engineering and Technology*, pp. 163-167, 50, 2009.

[5] Xin Wang Baofeng Tian, Chao Liang, Dongcheng Shil, “Blind image quality assessment for measuring image blur,” *Congress on Image and Signal Processing*, 2008.

[6] S. Mallat, *A Wavelet Tour of Signal Processing*, London Academic Press 1999.

[7] A. Serir and A. Belouchrani, “Multiplicative multiresolution decomposition with perfect reconstruction,” *IEEE ISSPIT, Darmstadt, Allemagne*, 14-17 Décembre 2003.

[8] A. Serir, A. Hamedène and F. Kerouh, “Blur Reduction by a multiplicative multiresolution decomposition MMD,” *Workshop on Systems, Signal Processing and their Applications*, Mai 2011, pp. 63 – 66.

[9] A. Serir and A. Belouchrani, “Multicative multiresolution decomposition for 2D signals: Application du speckle reduction in SAR images,” *IEEE ICIP*, Sangapour 24-25 October 2004.

[10] H. R. Sheikh, M. F. Sabir and A. C. Bovik, “A statistical evaluation of recent full reference image quality assessment algorithms,” *IEEE Transactions on Image Processing*, vol. 15, no. 11, pp. 3440-3451, Nov 2006.

[11] H. R. Sheikh, Z. Wang, I. K. Cormack, and A. C. Bovic. Live image Quality Assessment Database Release 2. [Online]. Available: http://live.ece.utexas.edu/research/qulity/subjective.htm

[12] Z. Wang, A. C. Bovik, H. R. Sheikh, and E. P. Simoncelli, “Image quality assessment from error visibility to structural similarity,” *IEEE Transactions on Image Processing*, vol. 13, no. 4, pp 600-612, April (2004).

[13] F. Kerouh and A. Serir, “A no reference quality metric for measuring image blur in the wavelet domain,” *IEEE, International Journal of Digital Information and Wireless Communication*, vol. 4, no. 1, pp. 767-776, 2012.

Fatma Kerouh was born in Jijel Algéria. She received the BE degree in electronics engineering from Mohamed Seddik Ben Yahia university, Jijel, Algeria on 2008, and the ME degree in intelligent and communicant systems at the university of Sciences and Technology Houari Boumediene, Algiers in 2010, where she is currently pursuing the P. h. D degree. Her current researches include images and video quality assassessment and restoration.

Amina Serir Benmrabet was born in Algiers**,** Algeria. She received an engineering degree in electrical engineering from state high school, Polytechnic School, Algiers on 1985. She had worked in the design office of Algeria airlines. Then she joined the University of Sciences and Technology and received in 2002, her PhD degree, in image processing. Since she has been head of the team of “2D and 3D image processing” of the labora laboratory of image processing and radiation LTIR of the Department of Telecommunications and contributed to the creation of a High School of Technology ENST (2010-2011). She leads several national research projects through the integration of biometrics in smart cards for bank payment or in intelligent video. Her research interests include information processing systems in particular compression and information representation and analysis